COBEM 2021 26th International Congress of Mechanical Engineering
ABCM Associação Brasileira de Engenharia e Ciências Mecânicas
November 22-26, 2021, Virtual Congress, Brazil

COB-2021-1717
A FIRST ESTIMATE OF THE DISPLACEMENT OF MONO ETHYLENE GLYCOL IN AN OIL PIPELINE USING COMPUTATIONAL FLUID DYNAMICS (CFD)

Nathália Roseane de Melo
Karen Danyele da Silva Vieira
Alessandro Romário Echevarria Antunes
Federal University of Pernambuco - UFPE. Agreste Academic Center (CAA). Caruaru-PE, Brazil
nathalia.roseane@ufpe.br
karen.vieira@ufpe.br
alessandro.antunes@ufpe.br

Darlan Karlo Elisiário de Carvalho
Federal University of Pernambuco - UFPE. Technology and Geosciences Center (CTG). Recife-PE, Brazil
darlan.ecarvalho@ufpe.br

Giselle Maria Lopes Leite da Silva
Petróleo Brasileiro S.A.
gisellelopes@petrobras.com.br

Abstract. *The use of chemicals in oil-producing wells, especially in the Brazilian Pre-Salt, is done to avoid or mitigate possible flow assurance problems (scale, asphaltenes, hydrates, corrosion, and H_2S, for example). The downhole injection of these products, such as scale inhibitors, is carried out through dedicated systems and most of these inhibitors use Mono Ethylene Glycol (MEG) as a solvent. In this research, the injection of MEG (scale inhibitor solvent) into an oil-water laminar flow was simulated using the commercial software Ansys® Fluent, Release 2021 R1, and Release 2021 R2, as a methodology to predict the mass fraction of this substance along with the flow and the effectiveness of the inhibition. A two-phase, two-component flow without chemical reactions and interfacial mass transfer was modeled, in which the primary phase consists of oil and the dispersed phase is formed by the MEG-water mixture. The results obtained allowed us to estimate the diffusion of the substance in the pipeline and to observe that, approximately from 2.5m away from the injection source, the mass fraction of the substance is lower than required for the proposed objective, but more numerical experiments and comparisons with real applications are needed to validate the adopted strategy.*

Keywords: *Flow Assurance Problems, Displacement of Mono Ethylene Glycol in Oil pipelines, Numerical Simulation.*

1. INTRODUCTION

In oil and gas production systems, the flow is normally composed of oil, scale solids, water, gas, among other substances, with physical-chemical properties forming distinct phases, which characterize the multi-phase flow, or with the mixture of completely miscible gases or liquids, characterizing the multi-component flow (Paiva, 2014) (Ajoko *et al.*, 2015). In these systems, when properties such as pH, temperature, pressure, and concentration of dissolved ions in the injected water are modified, the chemical equilibrium is disturbed, causing the precipitation of dissolved ions and the deposition of scale (Nergaard and Grimholt, 2010), a threat to flow assurance that has been an issue historically addressed in the search for effective methodologies to prevent and mitigate technical and economic losses from these phenomena, such as pipeline blockage, formation and equipment damage, premature abandonment of wells (Ko *et al.*, 2020) and the need to perform maintenance and equipment replacement (Vazirian *et al.*, 2016).

Inorganic scale is formed mainly by calcium carbonate and sulfate, barium and strontium sulfate, iron, silicon sediment, and other insoluble solids. They can occur in a single mineral phase or combination of different minerals, and are independent or sensitive to the pH of the brine, and are formed by homogeneous or heterogeneous nucleation (Olajire, 2015) when the concentration of the species is above the solubility limit (Gudmundson, 2018). Scale management can be accomplished through pH control methods, injection of scale inhibitors, or the use of nanofiltration membranes. Inhibitors are chemical reagents used to prevent the nucleation and growth of scale crystals (Cruz *et al.*, 2018) and consist

of active functional groups that can form weak or strong bonds with cations, crystal-forming nuclei, and scale crystals, and hold them in the aqueous phase to prevent deposition (Mazumder, 2018). It consists of a cost-effective and efficient method that can reduce to almost zero the occurrence of the phenomenon and requires a proper study to perform (Olajire, 2015), because the incorrect selection of this reagent can provide the acceleration and recurrence of the phenomenon and efficiency is due to the ability of this product to access the scale, whereas the parameter of affected surface/volume of inhibitor is a determinant of the cost-effectiveness (Kamal *et al.*, 2018). Most scale inhibitors use Mono Ethylene Glycol (MEG) as a solvent, a substance that is injected, as in the Brazilian Pre-Salt producing wells, through gas lift systems and dedicated systems. It is water-soluble and immiscible with crude oil, producing a two-phase and two-component fluid flow.

Solano (2010) and Volk (2013) performed experimental and numerical studies aiming to describe the miscible displacement of Mono Ethylene Glycol as thermodynamic hydrate inhibitor (THI) in a subsea jumper during a system restart operation. The numerical studies were developed in commercial simulators OLGA (1-D), Ansys® Fluent (2-D), and Star-CCM+ (3-D), modeling the multi-component flow of water-MEG without chemical reaction, in laminar regime, with the prediction of the mass fraction of the species throughout the equipment with full and half liquid loading, during variable time intervals.Kamari *et al.* (2015) performed the prediction of MEG injection also as THI, using the least squares support vector machine (LSSVM) method, analyzing the influence of thermodynamic and process conditions such as injection temperature, molecular and weight percent of the substance, and gas temperature.

Rojas-Figueroa and Fairuzov (2002) simulated the injection of corrosion inhibitor into a stratified and dispersed flow of crude oil and water in a pipeline, applying the liquid-liquid two-phase flow model, with interfacial mass transfer of the inhibitor from one phase to another, considering it miscible in both phases, in the stationary and transient regimes, and studying the effects of injection rate, interfacial mass transfer and degradation rate of the inhibitor in the pipeline. Azari *et al.* (2020) simulated the application of scale inhibitors (SI) in squeeze treatments, using squeeze software, performing a sensitivity study to optimize the injection rate.

In this study, Ansys® Fluent, Release 2021 R1, and Release 2021 R2 are used to perform the 3-D numerical simulation of the two-phase, two-component laminar and transient fluid flow from the injection of Mono Ethylene Glycol,used as a scale inhibitor solvent, into the oil-water mixture in a vertical pipeline as a methodology for the initial prediction of the mass fraction of this substance in the flow.

2. METHODOLOGY

Numerical simulation of four cases of the two-phase, two-component flow of Mono Ethylene Glycol (MEG) into the oil-water mixture in a 50 m long pipeline with an internal diameter equal to 0.12 m was performed. The oil/water flow is 2.48×10^{-2} m^3/s (BSW=36% - Water flow/Net flow), the mass diffusion coefficient is 4.2 $\times10^{-10}$ m^2/s, the MEG-water droplet diameter considered is 6.85×10^{-6} m, and the flow time is 600 s. The MEG inlet has a diameter of 1.01×10^{-2} m and is located perpendicular to the oil-water inlet, as shown in Fig. 1.

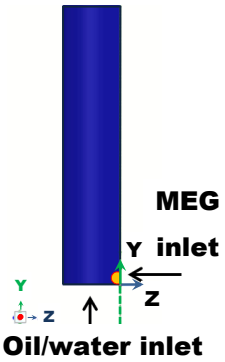

Figure 1. Schematic representation of the MEG and oil/water inlet in the pipe. Image used courtesy of ANSYS, Inc.

Table 1 shows the physical properties of Mono Ethylene Glycol (MEG), oil, and water.

Table 1. Physical properties of Mono Ethylene Glycol (MEG), oil and water.

Property	**MEG**	**Oil**	**Water**
Density (kg/m^3)	1.11×10^3	0.85×10^3	998.70
Viscosity (kg/m.s)	1.69×10^{-2}	5.66×10^{-3}	10^{-3}
Molecular weight (kg/mol)	6.21×10^{-2}	8.78×10^{-2}	1.80 10^{-2}
Reference temperature (K)	298.16	353.15	298

The injections analyzed occur according to the transient velocity profiles shown in Fig. 2.

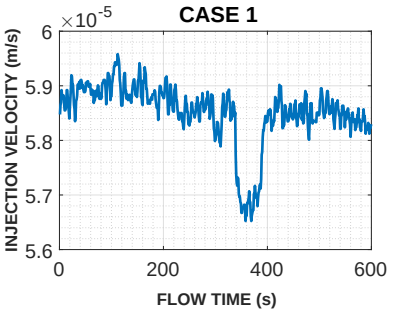

(a) Case 1, average injection velocity: 5.85×10^{-5} m/s.

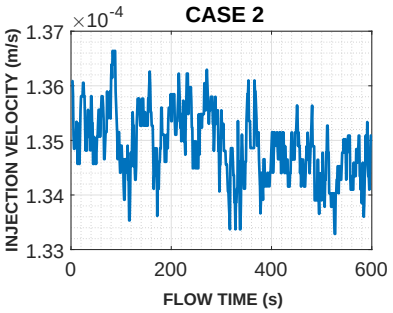

(b) Case 2, average injection velocity: 1.35×10^{-4} m/s.

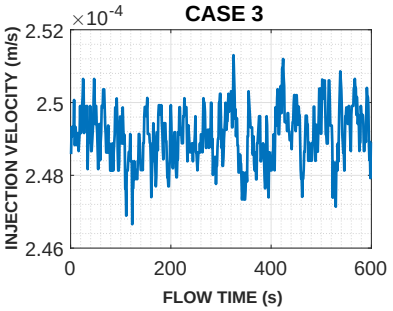

(c) Case 3, average injection velocity: 2.49×10^{-4} m/s.

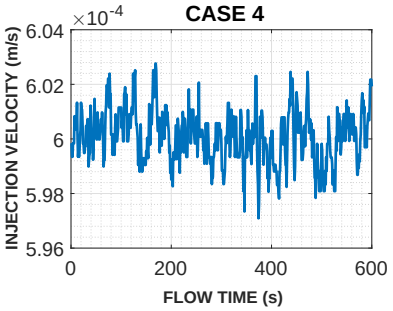

(d) Case 4, average injection velocity: 6.00×10^{-4} m/s.

Figure 2. Injection velocity transiente profiles.

Considering that MEG is soluble in water and insoluble in oil, the multi-phase mixture model was used to calculate the transport of oil, the primary phase, and the MEG-water mixture as the dispersed phase, and the multi-component species transport model without reaction was used to calculate the miscible displacement of Mono Ethylene Glycol in water. The pipeline cross-sections are considered to be inhibited from scale formation if they reach the mass fraction of MEG shown in Tab. 2.

Table 2. Produced water rate and required MEG mass fraction.

Case	Produced water rate (m^3/s)	Required MEG mass fraction
1	8.92×10^{-3}	6.23×10^{-5}
2	8.92×10^{-3}	1.56×10^{-4}
3	8.92×10^{-3}	3.11×10^{-4}
4	8.92×10^{-3}	7.47×10^{-4}

The boundary conditions for these simulations are:

MEG inlet: transient velocity profiles, temperature equal to 353.15 K, and MEG mass fraction equal, MEG-water volumetric fraction equal to 1.

Oil-water inlet: velocity equal to 2.21 m/s, temperature equal to 352.89 K, MEG mass fraction equal to 0, MEG-water volumetric fraction equal to 1.

Outlet: temperature equal to 352.82 K, gauge pressure equal to 3673269 Pa, backflow MEG mass fraction and backflow MEG-water volumetric fraction equal to 0.

Walls: temperature equal to 353.15 K, Stationary wall, no-slip, MEG diffusive flux equal to 0, adhesion angle equal to 90°.

At $t = 0$ s, MEG mass fraction and velocities in the x, y and z directions were set equal to 0, temperature equal to 352.89 K, and MEG-water volumetric fraction equal to 0.36 in the entire domain. A register of a 6-cell layer was originated from the MEG inlet, where the substance mass fraction and MEG-water mixture volumetric fraction equal to 1, were determined.

The operating conditions are the reference pressure equal to 37954208 Pa at $x = y = z = 0$ m, the temperature of 353.15 K, the gravitational acceleration equal to 9.81 m/s^2 in the y direction, and density of the multiphase mixture described by the minimum-phase-averaged.

2.1 Multiphase formulation: The mixture model

The mixture model (ANSYS, 2021) is a simplification of the Eulerian model, based on the assumption that the Stokes number,

$$St = \frac{\tau_d}{\tau_c} \tag{1}$$

is much smaller than one, being τ_d the ratio of the dispersed phase relaxation time, and τ_c the characteristic time scale of the flow. In this model the following equations are solved: mass continuity, momentum, and energy for the mixture and the volume fraction equation for the dispersed phases, and, if the phases move at different speeds, algebraic expressions for relative speeds are solved (ANSYS, 2021). Thus, the continuity equation for the mixture is:

$$\frac{\partial}{\partial t}(\rho_m) + \nabla \cdot (\rho_m \mathbf{v_m}) = 0 \tag{2}$$

in wich the mass-average velocity $\mathbf{v_m}$ is

$$\mathbf{v_m} = \frac{\sum_{k=1}^{n} \alpha_k \rho_k \mathbf{v_k}}{\rho_m} \tag{3}$$

where α_k, $\mathbf{v_k}$, and ρ_k are the volume fraction, the relative velocity, and the density of the phase k, respectively, and the mixture density ρ_m is expressed by

$$\rho_m = \sum_{k=1}^{n} \alpha_k \rho_k \tag{4}$$

The momentum equation of the mixture is equal to the sum of the momentum equations of the n phases. Thus,

$$\frac{\partial}{\partial t}(\rho_m \mathbf{v_m}) + \nabla \cdot (\rho_m \mathbf{v_m} \mathbf{v_m}) = -\nabla p + \nabla \cdot \left[\mu_m (\nabla \mathbf{v_m} + \nabla \mathbf{v_m^T})\right] + \rho_m \mathbf{g} + \mathbf{F} + \nabla \cdot \left(\sum_{k=1}^{n} \alpha_k \rho_k \mathbf{v_{dr,k}} \mathbf{v_{dr,k}} \right) \tag{5}$$

where $\mathbf{F}$ is the body force, the mixture viscosity is expressed by Eq. (6) and the drift velocity for secondary phase k ($\mathbf{v_{dr,k}}$) is the difference between $\mathbf{v_k}$ and $\mathbf{v_m}$.

$$\mu_m = \sum_{k=1}^{n} \alpha_k \mu_k \tag{6}$$

The mixture energy equation is expressed by Eq. (7), where k_{eff} is the effective conductivity, k_t is the turbulent thermal conductivity, and S_E is a volumetric heat sources term.

$$\frac{\partial}{\partial t} \sum_{k=1}^{n} (\alpha_k \rho_k E_k) + \nabla \cdot \sum_{k=1}^{n} (\alpha_k \mathbf{v_k} (\rho_k E_k + p)) = \nabla \cdot (k_{eff} \nabla T) + S_E \tag{7}$$

For compressible phase:

$$E_k = h_k - \frac{p}{\rho_k} + \frac{v_k^2}{2} \tag{8}$$

where h_k is sensible enthalpy for phase k. For incompressible phase:

$$E_k = h_k \tag{9}$$

For the relative velocity $\mathbf{v_k}$:

$$\mathbf{v_{pq}} = \mathbf{v_p} - \mathbf{v_q} \tag{10}$$

where $\mathbf{v_p}$ is the velocity of the dispersed phase, and $\mathbf{v_q}$ is the velocity of the continuous phase. For the drift velocity $\mathbf{v_{dr,p}}$, one has the expression (ANSYS, 2021):

$$\mathbf{v_{dr,p}} = \mathbf{v_{pq}} - \sum_{k=1}^{n} c_k \mathbf{v_{qk}} \tag{11}$$

and c_k is the mass fraction for phase k:

$$c_k = \frac{\alpha_k \rho_k}{\rho_m} \tag{12}$$

In the algebraic slip formulation, it is assumed that:

$$\mathbf{v_{pq}} = \frac{\tau_p}{f_{drag}} \frac{(\rho_p - \rho_m)}{\rho_p} \mathbf{a} \tag{13}$$

where τ_p is the particle relaxation time, and $\mathbf{a}$ is the secondary-phase particle's acceleration:

$$\mathbf{a} = \mathbf{g} - (\mathbf{v_m} \cdot \nabla)\, \mathbf{v_m} - \frac{\partial \mathbf{v_m}}{\partial t} \tag{14}$$

The Schiller and Naumann default drag function (ANSYS, 2021) is shown in Eq. (15).

$$f_{drag} = \begin{cases} 1 + 0.15Re^{0.687} & Re \leq 1000 \\ 0.0183Re & Re > 1000 \end{cases} \tag{15}$$

The volume fraction equation for secondary phase p is:

$$\frac{\partial}{\partial t}(\alpha_p \rho_p) + \nabla \cdot (\alpha_p \rho_p \mathbf{v_m}) = -\nabla \cdot (\alpha_p \rho_p \mathbf{v_{dr,p}}) + \sum_{q=1}^{n} (\dot{\mathbf{m}}_{\mathbf{qp}} - \dot{\mathbf{m}}_{\mathbf{pq}}) \tag{16}$$

where $\dot{\mathbf{m}}_{\mathbf{qp}}$ and $\dot{\mathbf{m}}_{\mathbf{pq}}$ are source terms for interphase mass transfer, and are not considered in this study.

2.2 Multi-component formulation: The species transport model without reactions

In multi-component systems, with concentrations that vary at each point, there are mass flows that occur by molecular diffusion and convection (Livi, 2004). Using the species transport model (ANSYS, 2021), the mass conservation equation, which is solved for $N-1$ species in a mixture, where N is the number of species, can be written, as:

$$\frac{\partial(\rho Y_i)}{\partial t} + \nabla \cdot (\rho \mathbf{v} Y_i) = -\nabla \cdot \mathbf{J_i} + R_i + S_i \tag{17}$$

where $\mathbf{v}$ is the mass velocity, R_i is a source term for the production of species i by chemical reaction, S_i is a user-defined source term, $\mathbf{J_i}$ is the diffusive flow of the species, and Y_i is the mass fraction of the species. For laminar flows, one has:

$$\mathbf{J_i} = -\rho D_{i,m} \nabla Y_i - D_{T,i} \frac{\nabla T}{T} \tag{18}$$

where $D_{i,m}$ is the mass diffusion coefficient of the species and $D_{T,i}$ is the thermal diffusion coefficient. In the model (ANSYS, 2021) one also considers the transport of enthalpy due to species diffusion, where one has:

$$\nabla \cdot \left[\sum_{i=1}^{n} h_i \mathbf{J_i} \right] \tag{19}$$

In this study, it is considered that the multi-component phase properties of the density and the specific heat capacity, are described by volume-weighted-mixing-law and mixing-law, respectively, and the thermal conductivity and the viscosity are described by mass-weighted-mixing-law.

2.3 Numerical formulation

Considering gravity acting symmetrically on the vertical pipeline cross-section, a discretization of half of the pipe was performed using an unstructured mesh with 393164 tetrahedral elements, Fig. 3. The reference mesh for this problem has 1110609 finite volumes.

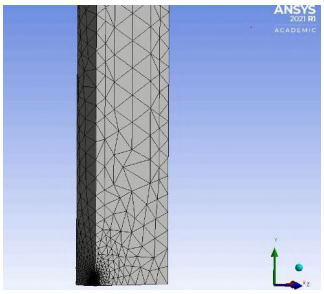

Figure 3. Representation of a mesh section. Image used courtesy of ANSYS, Inc.

The implicit formulation for the volume fraction equation and the volume fraction cutoff equal to 4.20 $\times 10^{-6}$ was assumed. The slip velocity of the secondary phase (MEG-water mixture) was described using the algebraic method of

Manninen *et al.* (1996) and the drag function of Schiller and Naumman was selected. Implicit body force was enabled to include body force correction terms in the cell pressure correction. There are no effects of mass transfer and chemical reactions.

The advective terms of the momentum, convection-diffusion, and energy equations were discretized through second-order upwind and the advective terms of the volume fraction equation were discretized by the QUICK method. The diffusive terms were discretized through central-differenced. To perform the pressure-velocity coupling, the couple method was used, gradients were calculated from the Cell-Based Least Squares method and to estimate the pressure field at the mesh faces, PRESTO! (PREssure STaggering Option) was used. The time-dependent terms were discretized using the implicit first-order formulation. A three order of magnitude reduction of the residuals of the mass fractions of Mono Ethylene Glycol and water and the velocities in x, y, and z were set as the convergence criterion.

3. RESULTS AND DISCUSSIONS

The mass fractions of MEG in the pipeline at flow time instants of 5, 15, 30, 60, 120, 300 and 600 s were analyzed, Fig. 4. It can be seen that in all cases and time instants analyzed, before 2.5 m away from the injection point (approximately), the mass fraction of the substance is above what is required for inhibition, and from this point on, all sections are subinhibited.

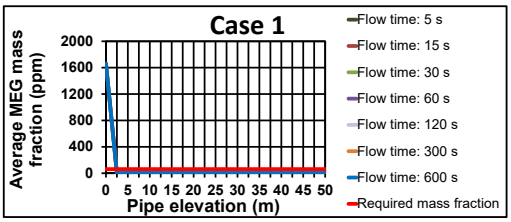

(a) Case 1, average injection velocity: 5.85×10^{-5} m/s.

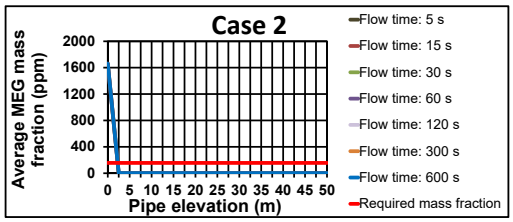

(b) Case 2, average injection velocity: 1.35×10^{-4} m/s.

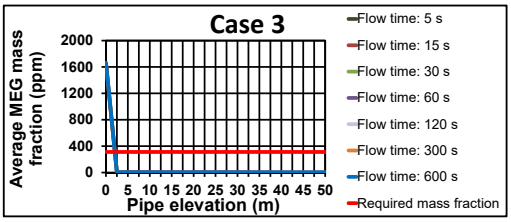

(c) Case 3, average injection velocity: 2.49×10^{-4} m/s.

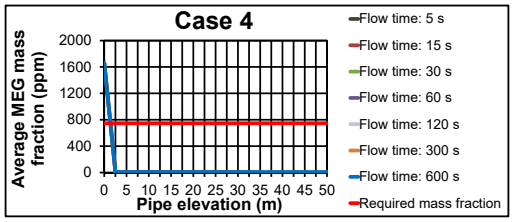

(d) Case 4, average injection velocity: 6.00×10^{-4} m/s.

Figure 4. MEG mass fraction (ppm).

From $y = 2.5$ m, the MEG-water mixture becomes very dilute, and the referred fraction assumes values less than 10 ppm, as shown in Fig. 5. It is found that flow reaches the stationary regime from $t = 60$ s.

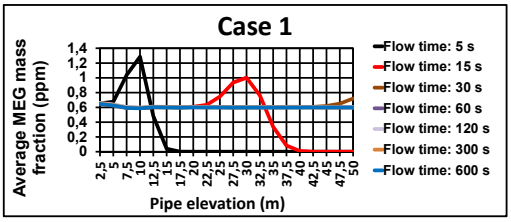

(a) Case 1, average injection velocity: 5.85×10^{-5} m/s.

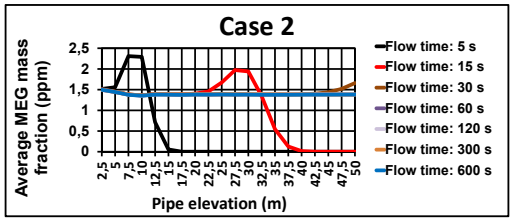

(b) Case 2, average injection velocity: 1.35×10^{-4} m/s.

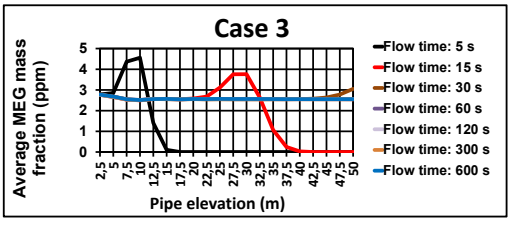

(c) Case 3, average injection velocity: 2.49×10^{-4} m/s.

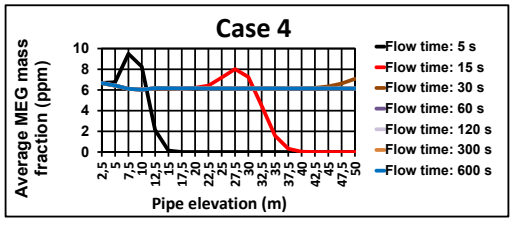

(d) Case 4, average injection velocity: 6.00×10^{-4} m/s.

Figure 5. MEG mass fraction (ppm).

As the injection rate increases, so do the difference between the required mass fraction and the average predicted fraction from $y = 2.5$ m, Fig. 6.

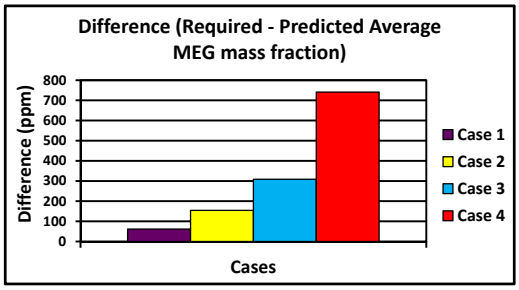

Figure 6. Difference (Required - Predicted MEG mass fraction).

From Fig. 7(a) it is seen that the mass fraction of the substance, regardless of the injection rate and flow time, always remained equal to approximately 1660 ppm. In Fig. 7(b) it is observed that it takes 15 s for the substance to reach $y = 50$ m.

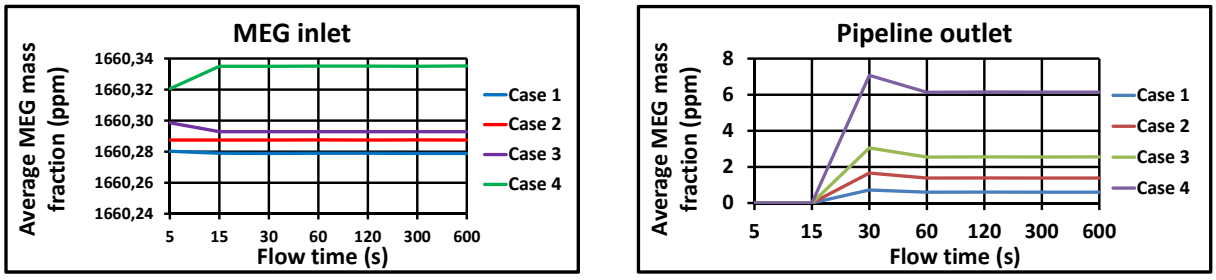

(a) MEG inlet. (b) Pipeline outlet.

Figure 7. MEG mass fraction (ppm) - MEG inlet and pipeline outlet.

The Figure 8 shows color maps of the pipeline cross section at $y = 2.5$ m and $y = 50$ m, at $t = 600$ s case 1 and case 2.

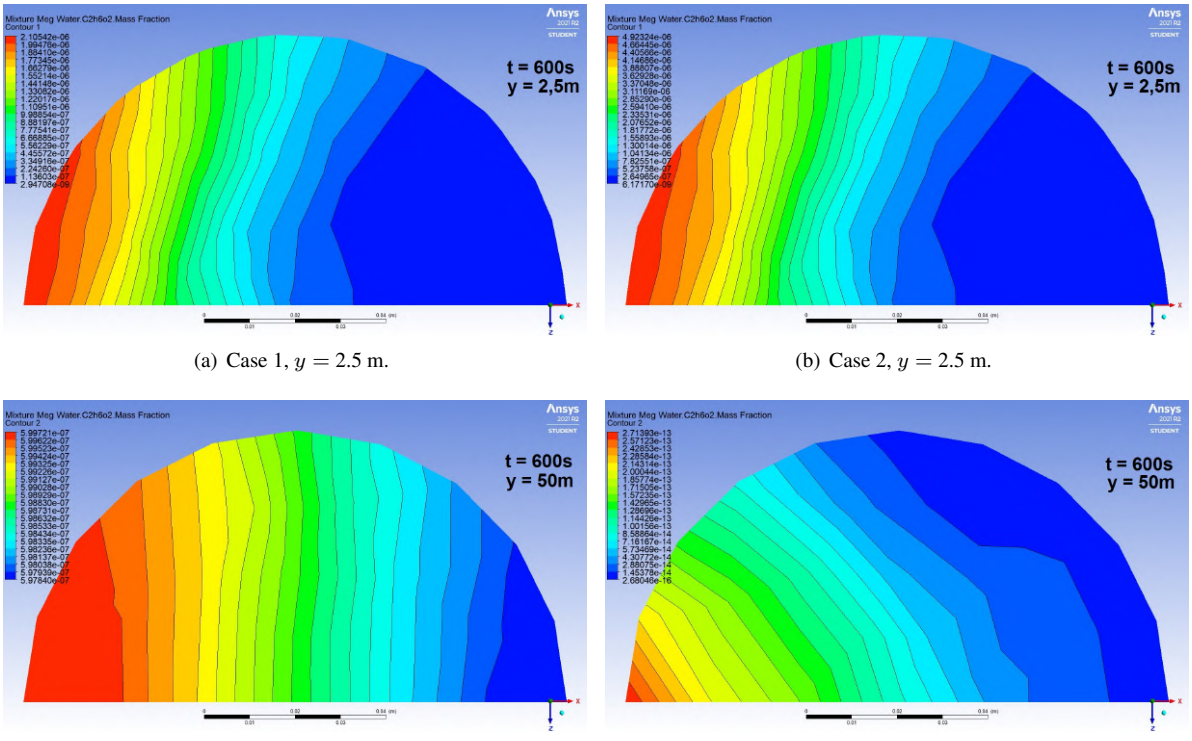

(a) Case 1, $y = 2.5$ m. (b) Case 2, $y = 2.5$ m.

(c) Case 1, $y = 50$ m. (d) Case 2, $y = 50$ m.

Figure 8. MEG mass fraction color maps (transversal sections).

The Figure 9 presents color maps of the longitudinal section of the pipeline from $y = 0$ m and from $y = 2.5$ m, at $t = 600$ s, case 1 and case 2.

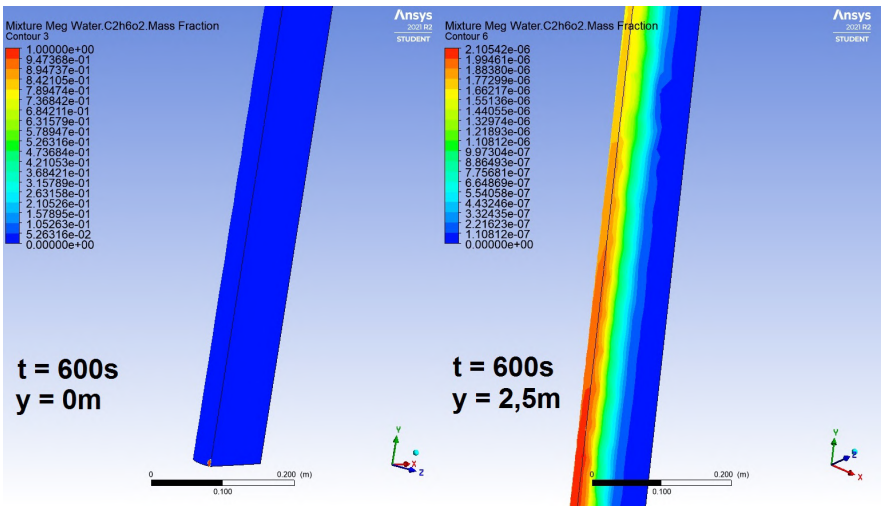

(a) Case 1, average injection velocity: 5.85×10^{-5} m/s.

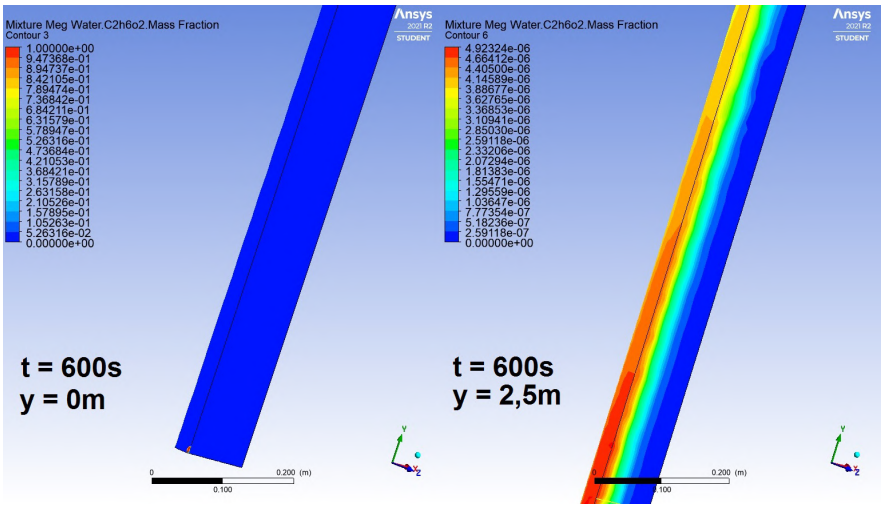

(b) Case 2, average injection velocity: 1.35×10^{-4} m/s.

Figure 9. MEG mass fraction color maps (longitudinal sections).

In Fig. 8 and Fig. 9 it is possible to analyze how the diffusion of Mono Ethylene Glycol occurs in the pipeline, always having a greater amount of the substance on the same side where the injection is performed.

The Figure 10 shows the prediction of the MEG mass fraction for Case 1, using the reference mesh.

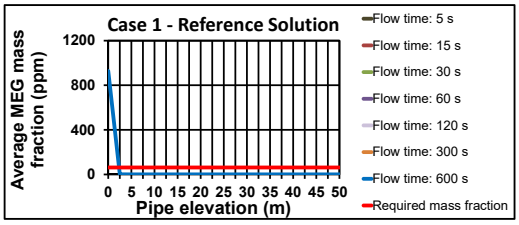

(a) Prediction of the mass fraction in the complete pipeline.

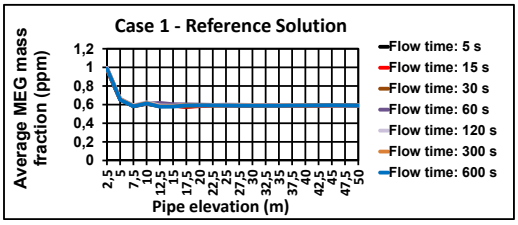

(b) Prediction of the mass fraction from $y = 2.5$ m.

Figure 10. Case 1: MEG mass fraction (ppm) - reference solution.

As with the cases analyzed previously, the simulation results with the reference mesh demonstrate that up to approximately $y = 2.5$ m, the referred mass fraction remains higher than required for scale inhibition, and from this point, the duct sections are subinhibited.

Figure 11(a) demonstrates the MEG mass fraction at the MEG inlet for case 1, comparing the solution obtained earlier with the one obtained through the reference mesh and Figure 11(b) checks the solutions of the same case at the pipeline

outlet.

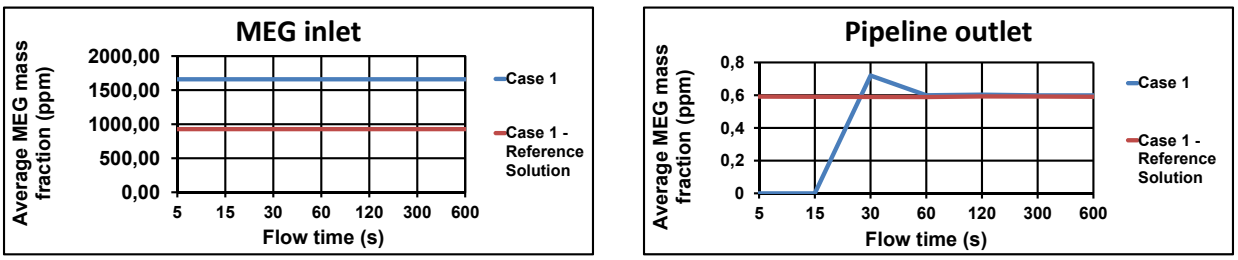

(a) Prediction of the mass fraction in the complete pipeline.

(b) Prediction of the mass fraction from $y = 2.5$ m.

Figure 11. Case 1: MEG mass fraction (ppm) - initial and reference solution at the MEG inlet and pipeline outlet.

With the reference mesh, 733.06 ppm less fraction was predicted than the initial solution for the MEG inlet. At the output of the pipeline, the reference solution predicts that at $t = 5$ s there is MEG at this location. Starting at $t = 60$ s, the mass fraction converges to the same value in both solutions.

4. CONCLUSIONS

The injection of Mono Ethylene Glycol into an oil-water flow was modeled to predict the MEG mass fraction, and verify if the average predicted fraction meets the amount required for the scale inhibition effect. According to the results obtained, the pipeline is subinhibited from $y = 2.5$ m, a condition that favors the formation of incrustations in this stretch. As the injection rate increases, the more difference there is between the required value and the average predicted value.

In all the cases, higher concentrations of the substance were always obtained on the same side where the injection is carried out. In the initial solutions, regardless of the injection rate, the average fraction referred to is approximately equal to 1660 ppm in the MEG inlet, while in the solution obtained through the reference mesh for case 1, 733.06 ppm less than this average value was predicted.

These initial solutions predict that 15 s are required for the substance to reach the pipeline outlet, while in the reference solution, at $t = 5$ s, 0.6 ppm of the mass fraction was predicted at this location. Both solutions converged to the same average value at $t = 60$ s.

It is emphasized that the modeling performed proposed an initial methodology to evaluate the effectiveness of the diffusion of this substance in pipelines and needs further numerical experiments and application studies in real scenarios to validate the adopted prediction strategy.

5. ACKNOWLEDGEMENTS

We express our thanks to the National Council for Scientific and Technological Development - CNPQ, the Postgraduate Program in Civil and Environmental Engineering - PPGECAM, the Petroleum and Energy Research Institute - LITPEG, the High-Performance Processing Group in Computational Mechanics (PADMEC), the Department of Special Collections and University Archives of the University of Tulsa and to the Mr. Sanjav Gaikwad, assistant professor of the Army Institute of Technology from Pune, India.

6. REFERENCES

Ajoko, T., Petro, N. and Nangi, E., 2015. "Multiphase flow simulation of oil and gas in vertical flow using cfx and fluent". *International Journal of Scientific and Engineering Research*, Vol. 6.

ANSYS, I., 2021. *Ansys® Fluent, Release 2021 R1, Theory Guide*. ANSYS, Inc, U.S.A.

Azari, V., Vazquez, O., Mackay, E.J., Sorbie, K., Jordan, M. and Sutherland, L., 2020. "Squeeze design optimization by considering operational constraints, numerical simulation and mathematical modelling". *SPE Virtual International Oilfield Scale Conference and Exhibition*.

Cruz, C., Kraslawski, A. and Cisternas, L.A., 2018. "Scaling problems and control technologies in industrial operations: Technology assessment". *Separation and Purification Technology*, Vol. 207.

Gudmundson, J.S., 2018. *Flow Assurance Solids in Oil and Gas Production*. CRC Press/Balkema, London, UK.

Kamal, M.S., Hussein, I., Mahmoud, M., Sultan, A.S. and Saad, M.A.S., 2018. "Oilfield scale formation and chemical removal: A review". *Journal of Petroleum Science and Engineering*, Vol. 171, pp. 127–139.

Kamari, A., Bahadori, A., Mohammadi, A.H. and Zendehboudi, S., 2015. "New tools predict monoethylene glycol injection rate for natural gas hydrate inhibition". *Journal of Loss Prevention in the Process Industries*, Vol. 33, pp. 222–231.

Ko, S., Wang, X., Zhao, Y., Dai, C., Lu, A.Y., Deng, G., Paudyal, S., Mateen, S., Kan, A.T. and Tomson, M.B., 2020.

"Prevention of mineral scale deposition using dispersants and inhibitors". In *SPE Virtual International Oilfield Scale Conference and Exhibition*.

Livi, C.P., 2004. *Fundamentos de Fenômenos de transporte: Um texto para Cursos Básicos, 2.ed.* LTC - Livros Técnicos e Científicos Editora S.A., Rio de Janeiro.

Manninen, M., Taivassalo, V. and Kallio, S., 1996. *On the mixture model for multiphase flow*. VTT Publications 288, Finland.

Mazumder, M.A.J., 2018. "A review of green scale inhibitors: Process, types, mechanism and properties". *Coatings*, Vol. 10, No. 10.

Nergaard, M. and Grimholt, C., 2010. "An introduction to scaling causes, problems and solutions".

Olajire, A.A., 2015. "A review of oilfield scale management technology for oil and gas production". *Journal of Petroleum Science and Engineering*, Vol. 135, pp. 723–737.

Paiva, A.S.S., 2014. *Escoamento de fluidos bifásicos em empacotamentos geométricos*. Master's thesis, Instituto de Física da Universidade Federal da Bahia, Salvador.

Rojas-Figueroa, A. and Fairuzov, Y.V., 2002. "Numerical simulation of corrosion inhibitor transport in pipelines carrying oil-water mixtures". *Journal of Energy Resources Technology*, Vol. 124, pp. 239–245.

Solano, S.D.M., 2010. *Experimental and computational investigation on the displacement and mixing mechanisms in well-head jumpers during restart with monoethylene glycol*. Master's thesis, The Graduate School of University of Tulsa, OK.

Vazirian, M.M., Charpentier, T.V.., de O Penna, M. and Neville, A., 2016. "Surface inorganic scale formation in oil and gas industry: As adhesion and deposition processes". *Journal of Petroleum Science and Engineering*, Vol. 137, pp. 22–32.

Volk, M., 2013. "Displacement mixing in subsea jumpers - experimental data cfd simulations". Research Partnership to Secure Energy for America, RPSEA, edx.netl.doe.gov/dataset/displacement-mixing-in-subsea-jumpers-experimental-data-and-cfd-simulations-fact-sheet. Accessed 16 October 2020.